# A FEATURE-BASED DECISION-MAKING APPROACH (FBDMA) FOR TUMOR DETECTION USING DEEP LEARNING

P. Durga[1]
[1]Research Scholar, School of Computer Science and Engineering,
VIT-AP University, Amaravati, AP, India
Email: pdurga593@gmail.com

Dr. T. Sudhakar[2*]
[2]Associate Professor, School of Computer Science and Engineering,
VIT-AP University, Amaravati, AP, India
[*]Corresponding author mail: tsudhakar105@gmail.com

**Abstract**

**Nowadays diseases become more dangerous to people. Diseases are of many types such as infections, viruses, etc. Some types of infections are converted to tumors. Tumors are very dangerous to humans that can occur anywhere in the human body. Generally, people are suffering from various tumors that may or may not convert to cancers. It is very important to find the tumors in the body and analyze the tissues in the early stages. Tumors are of several types Benign, Premalignant, and Malignant. Among those types benign is not cancer and malignant is cancer. Deep Learning (DL) algorithms are one of the significant approaches that can find tumors in the human body. Several drawbacks are identified with the existing models such as this will not support large datasets, no image filtering is used, and supports only limited features from input images. A feature-based decision-making approach (FBDMA) is proposed to detect tumors in any body parts of human beings. The proposed approach FBDMA is combined with the pre-trained model VGG19 which consists of 19 layers for better training. The preprocessing technique is used to remove the noise from the input images. Image filters are used to remove the continuous noise from the input images. Convolutional neural network (CNN) is applied to feature extraction and classify tumors and non-tumors. FBDMA is used to classify the cancerous and non-cancerous images that are collected from CNN layers. The FBDMA is applied to MRI brain tumor datasets that are collected from online sources such as https://www.kaggle.com/ahmedhamada0/brain-tumor-detection. The performance is analyzed by showing different performance metrics such as sensitivity, precision, recall, and f1-score. And the performance is compared with related existing systems and the proposed system achieved high performance with an accuracy of 98.67 in detecting cancer cells.**

***Keywords*: Deep Learning (DL); tumors; feature-based decision-making approach (FBDMA); cancer; non-cancer.**

## 1. Introduction

In the healthcare systems deep learning (DL) plays a significant role to predict diseases very efficiently [1]. Working on tumors becomes more complicated for the existing algorithms or models. There are 120 types of brain tumors are present. Some tumors are growing very fast and some tumors are slow-growing. Fast-growing tumors are most dangerous to people of all ages and may become cancers. It is very difficult for experts to detect the tumor stages automatically [2]. Non-communicable diseases (NCDs) become more serious health issues that lead to the cause of death. For the past many years, artificial intelligence (AI) based systems are developed with decision-making approaches to reduce the severity of disease prediction [3]. Computer-based clinical decision support systems (CDSSs) are the other decision-making approach that addresses the various issues in disease prediction [4]. The CDSS can be applied to various tumors that diagnose the disease stages.

There are several automated brain tumor approaches are developed such as content-based image retrieval (CBIR) to detect tumors in the brain. This approach mainly observes the difference between extracting low-level and high-level visual data from MRI brain images [5]. To reduce the gaps, these levels are used. Edge computing is most used in predicting diseases with the integration of Internet of Things (IoT) devices [6]. To find the accurate edges of the tumors edge-based approaches are used. Generative Adversarial Networks (GAN) are the model used to detect tumors from high-quality images [7]. The convolutional neural network (CNN) plays a significant role in training the MRI scan brain tumor images for extracting the quality features.

Several methods such as segmentation, extraction, and detection from MRI images find the tumor regions. Segmentation is the process that separates the cerebral venous system with the addition of a fully automated algorithm [8]. Tumor segmentation combined with CNN gives a better output. The two segmentation networks such as 3D CNN and U-Net give better results for accurate results for the prediction of tumor regions and these models achieved accurate tumor-detected regions [9]. Another deep learning (DL) approach VGG Stacked Classifier Network (VGG-SCNet's) [10] is used for the segmentation of MRI images and classify the brain tumors using neural networks. But there are some limitations for VGG-SCNet's such as this is not suitable for benchmark datasets and this model taking more time for computation.

In this paper, we proposed FBDMA to overcome the drawbacks in [10]. The proposed system mainly focused on analyzing the tumors in the human brain. Presently DL is most widely used in many complex applications in many ways. DL algorithms mainly focus on processing enormous data and reducing the computation time. The pre-trained model finds the disease patterns from input images. The advanced filters identify the noise from input images and give high-resolution output images. This paper uses high-resolution images obtained from noise filters to detect tumors. FBDMA is the classification approach that can classify cancerous and non-cancerous tumors according to the analyzed properties of tumors. The reinforcement learning algorithm is incorporated to increase the proposed system's performance. This learning algorithm improves the tumor detection rate and detects the accurate regions of the tumors. Figure 1 architecture diagram of FBDMA for the detection and recognition of typical tumors and cancerous tumors.

The literature survey explains in section 2 several existing approaches belonging to DL models that are applied to predict the disease. The drawbacks and performance of these algorithms are also included in this section. Section 3 explains the proposed methodology with pre-trained model VGG-19, segmentation with optimal threshold, and CNN. In the same section, bilateral filter and FBDMA are defined. Section 4 describes the implementation results and discussions, and last section 5 contains the conclusion.

## 2. Literature Survey

Y. Zhang et al., [11] proposed a cyber-physical system (CPS) for the development of a patient-centric healthcare system called Health-CPS. This system is combined with the cloud and big data. The proposed approach is the collection of multiple layers. Performance of the CPS achieved good results compared with previous approaches. S. Trajanovski et al. [12] proposed the semantic segmentation approach for the segmentation of tumors present in the tongue. The proposed approach, combined with the HSI data, gives accurate results. D. Hyun et al. [13] developed the 4-layer CNN to detect the adherent MB signatures. 4-layer CNN is a dual-mode channel approach that performed better than existing approaches. D. Krijgsman et al. [14] proposed the DL approach to classifying tumors from the breast. The author developed the CD8-positive cell detection algorithm consisting of various cancer tissues in the breast MRI images. The proposed approach also focused on detecting high-density regions. Y. Xie et al. [15] proposed the multi-view knowledge-based collaborative (MV-KBC) DL model that divides the malignant tumor cells from the chest CT data. The 3D lung nodule approach analyzed the properties of chest images. A KBC developed three types of image patches with the help of ResNet-50 networks to increase the detection rate. Finally, this model achieved better results by showing accurate results. A. S. Musallam et al. [16] introduced the three steps preprocessing approach (PPA) that works better on MRI images. The PPA used the DCNN to diagnose glioma, meningioma, and pituitary. In this model, significantly fewer layers are present, also called a lightweight model. The accuracy of the PPA achieved the 99%.

S. E. Divel et al., [17] proposed a framework that reduces the noise from the given input image with the local noise power spectra (NPS). By using the Fourier transform the image is filtered with the small patches with the square root with the spatial correlation. By using the standard deviation the patches are overlapped by using the spatially correlated noise. P. K Mallick et al., [18] introduced the image compression technique utilizing a DWA used to merge the default reduction approach adopted with auto-encoder to decompose the image of the wavelet transform. The classification is done by using DNN with the DWA. Compare with DNN the DWA-DNN shows better accuracy compared with existing techniques. N. Noreen et al., [19] introduced the method by extracting the multi-level features used to diagnose brain tumors in the early stages. Inception-v3, a pre-trained model integrated with the proposed classification gives better feature-based detection. Here, the two pre-trained models such as Inception-v3 and DensNet201 are used to improve the performance with the classification method.

A. Gumaei et al. [20] introduced a hybrid system to extract the features using the RELM to classify brain tumors. The preprocessing technique min-max normalization is used to improve the contrast of brain MRI image edges and locations. Then for the classification, the RELM is utilized. The proposed method shows better accuracy for classification compared with the existing techniques.

M. Li et al., [21] introduced the combined approach called multi-model fusion and CNN technique to detect brain tumors. This approach is an extension of 2D-CNN to 3D-CNN that can extract brain lesions utilizing various model properties of 3D space. Several dynamic layers such as the pooling layer and softmax layer are integrated with the proposed approach and achieve better performance. The loss function in this is used to improve the enhanced feature learning of the lesion region. The accuracy is improved when compared with the 2D-CNN. X.

Dong et al., [22] proposed the HFCNN used for the segmentation of liver tumors. This approach helps the patient to detect liver cancer. For the analysis of liver cancer, the HFCNN is used very effectively.

M. S. Majib et al., [23] proposed the VGG Stacked Classifier Network (VGG-SCN) to find tumors from MR images. VGG-SCN classifies the tumor or non-tumor images without any human interference. The proposal solves several issues such as reducing time-consuming and increasing accuracy. P. Khan et al., [24] introduced a new study about various brain diseases such as AD, brain tumors, Parkinson's disease, etc. Several pre-processing techniques, pre-trained models, and feature extraction techniques are discussed in this study. In this research, 22 datasets are also analyzed to diagnose brain diseases. A. Anaya-Isaza et al., [25] proposed the dynamic learning system (DLS)combined with data augmentation and transfer learning. ResNet50 is a pre-trained network used to detect effective tumors. Y. Zhang et al., [26] discussed the tumors that are present in the liver. The CT scan images are used for the detection of tumors in the liver. A novel level-set approach is used to refine the segmentation in tumors. FCM clustering is used for the probabilistic distribution of the liver tumor. This approach is applied to two datasets and segmentation is performed.

Z. Zhang et al., [27] address the various stages in the detection of tumors that occur during pregnancy. The author developed the ML map to process the tumors using a logistic regression classifier (LRC) and CNNs. Here, ultrasound scan images are used for the experimental analysis. M. Valkonen et al., [28] detected the tumors present in the breast. A pre-trained D-CNN is used for fine-tuning the dataset images. Most training is mainly applied to detect the carcinoma cells in the breast and these are considered cancer cells. C.-M. Feng et al., [29] proposed a new PCA approach that reduces the loading for the proposed approach. The proposed approach is called supervised discriminative sparse PCA (SDSPCA). The proposed approach mainly focused on reducing sparsity and increasing classification accuracy. The performance of the SDSPCA achieved better accuracy. Based on the performance the accuracy is improved. J. Sun et al., [30] introduced an algorithm to detect the weld and classification based on the dataset. The gaussian mixture model (GMM) is used to extract the features based on weld defects. Better performance is analyzed with the proposed approach.

Table 1: CIFAR-10 Confusion Matrix

| **Authors** | **Training Model/Feature Extraction** | **Proposed Model** | **Dataset** | **Performance Metrics** |
|---|---|---|---|---|
| Y. Shi et al., [31] | Coupled-based feature extraction | Novel coupled boosting model | Alzheimer's Disease Neuro-imaging Initiative (ADNI) | ACC, Sen, Spc, AUC |
| X. Bai et al., [32] | Advanced training | An improved possibilistic fuzzy c-means (FCM) | IBSR_20 Normal's | Accuracy |
| M. A. Ottom et al., [33] | Random Training Approach | Znet Model | TCGA - LGG | ACC, Sen, Spc, AUC |
| S. Asif et al., [34] | InceptionResNetV2 | Xception architecture using ADAM optimizer | MRI-Large and small dataset | ACC, Sen, Spc, Precision |
| N. Noreen et al., [35] | Inception-v3 and DensNet201 | multi-level features extraction | T1-weighted contrast MR images | ACC, Sen, Spc, Precision |
| S. Ahmad et al., [36] | VGG-16, VGG-19 | deep learning-based feature extractor and classifier | MRI dataset from Kaggle | ACC, Sen, Spc, Precision |
| Q. Hao et al., [37] | 2D-CNN-based spectral-spatial HSI feature extraction and classification | Edge-preserving filtering-based classification result fusion and optimization | Imagenet datasets | ACC, Spc, and F1 Score |
| H. A. Shah.,[38] | Convolution neural network (CNN) | D-CNN + EfficientNet-B0 base model | Two real human brain hyper-spectral datasets | Pre, Recall, ACC, Spc, and F1 Score |
| A. H. Abdel-Gawad.,[39] | Optimum Thresholding Algorithm | BCET | MR brain Images datasets | Mean, STD, Variance, Entropy |
| Z. A. Al-Saffar.,[40] | GLRLM | MI-ASVD | MRI Dataset collected from TCIA (The Cancer Imaging Archive) | Sen, Spc, and Acc |

## 3. Proposed Methodology: FBDMA

This paper proposed a Feature Based Decision-making Approach to detect tumors in any body part of human beings. It follows several steps for detecting the tumor cells.
A. VGG 19 pre-trained model
B. Optimal Threshold
C. CNN
D. Bilateral Filter
E. Identification of Cancer Cells
We used the VGG19 pre-trained for feature extraction on the ImageNet dataset. For the segmentation of the images, we use the Optimal threshold to find the unique regions in the input MRI images, and CNN is used for the effective classification of tumor images after that tumor images are given as input for the detection of cancer cells. Figure 2 explains the step-by-step process to find the tumors in brain MRI images. We want to remove the noise in tumor images by using advanced image filters such as the Bilateral filter (BF). The functionality of BF is to reduce the noise by smoothing the images to get noise-free tumor images. Then, we applied our FBDMA approach to identify the cancer cells' location and detect the cancer cells from the given tumor images. Automatic detection of brain tumors will make it easier for doctors and nurses to determine the type of tumor a patient has and start treating them immediately.

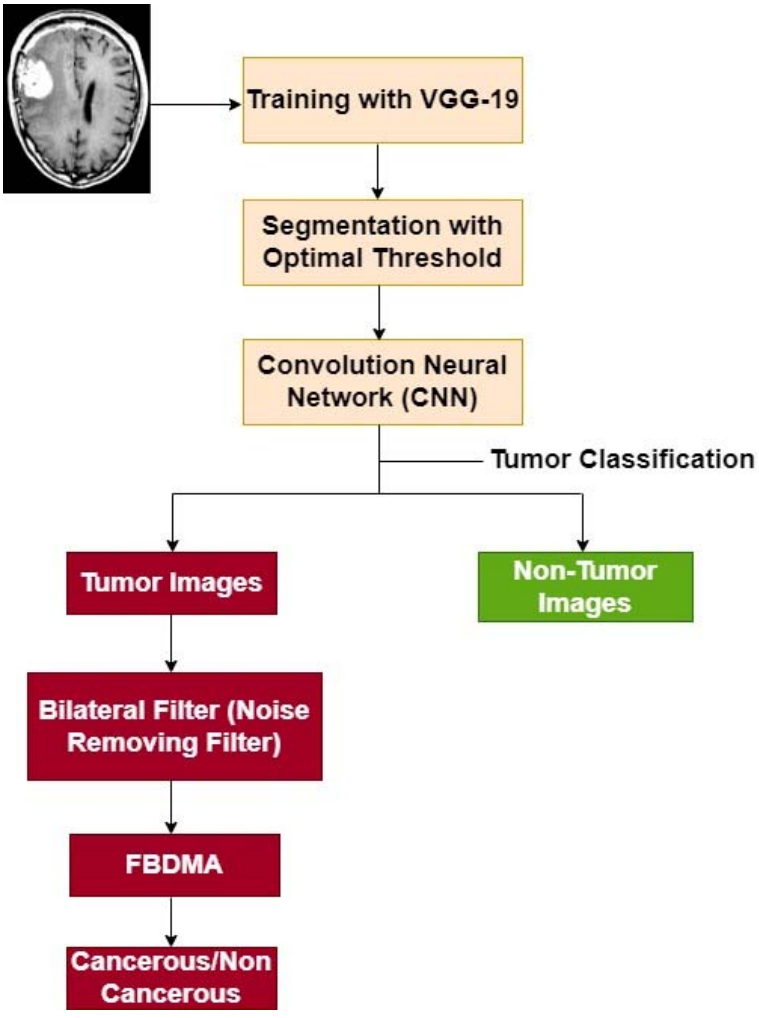


Fig. 1. Architectural Diagram for FBDMA

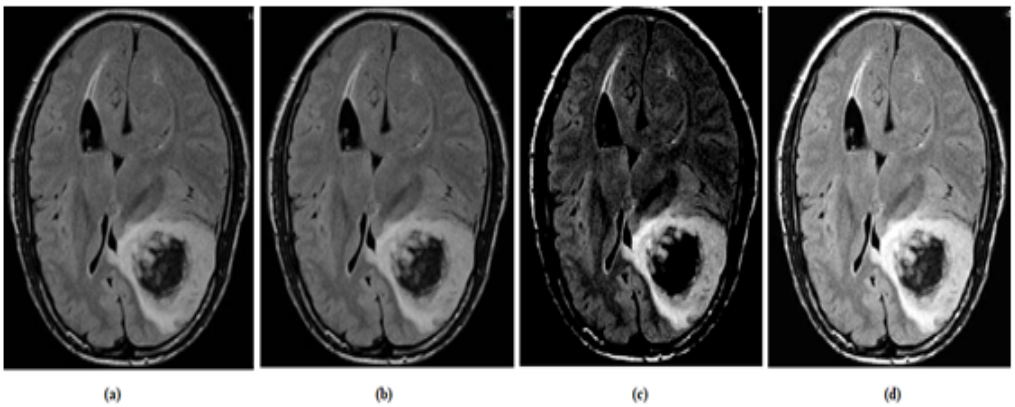


Fig. 2. Input MRI Brain Image, (b) Noise Removal Image, (c) Segmented Image, (d) Optimal Threshold Tumor image

### *3.1 VGG 19 pre-trained model*

VGG-19 is a pre-trained model used as training for the given input images. This model consists of 19 layers with 3 x 3 Convolution filters and a stride of 1 developed to obtain high accuracy in huge-scale image applications. VGG19 is required in this work because it is a very powerful model to extract the large-scale feature extractor with high accuracy. In this paper, VGG19 is used to increase the accuracy of classification for brain tumors.
In this model, the 19 layers are divided as 16 layers are convolutional layers utilized to extract the features and 3 layers work on image classification. The layers that are used for feature extraction are divided into 5 groups and every group is named a max-pooling layer. The input size of the image is 224 x 224 and the output of the model shows the object in the image. Fig 3 shows the structure of the VGG19 model.

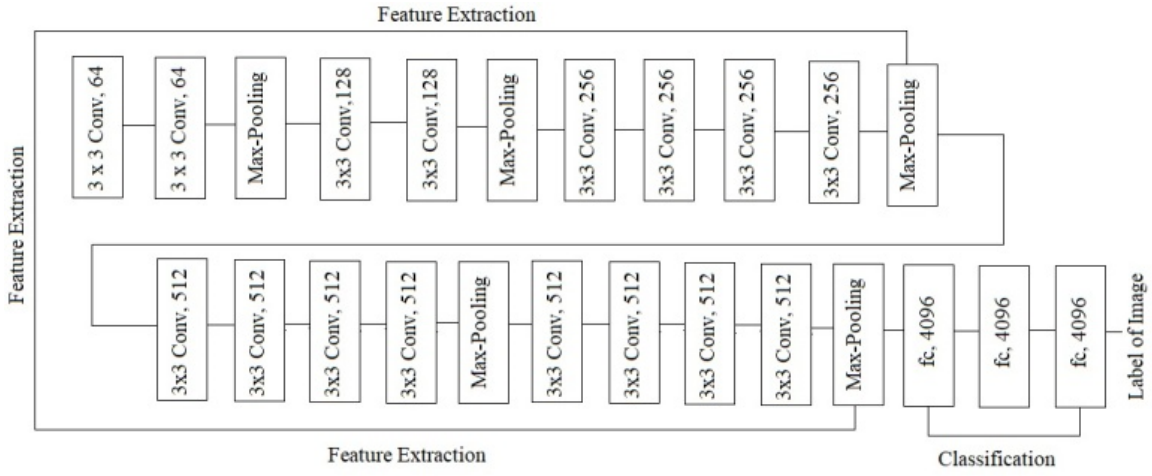


Fig.3. VGG-19 Architecture for Pre-Trained and Feature Extraction

### *3.2 Segmentation with Optimal Threshold*

Image threshold is the approach utilized to predict the threshold values and finds the unique regions in the input MRI image. An optimal threshold is utilized to reduce the misclassification of pixels based on segmentation. By using the iterative technique the misclassification loss of a pixel is measured by using the optimal threshold.

$$\mathrm{Prob}(X) = \mathrm{Prob}_1 * p_1(X) + \mathrm{Prob}_2 * p_1(X) \Rightarrow \mathrm{Prob}_1 + \mathrm{Prob}_2 = 1 \quad (1)$$

$$p_1(X) = \text{PDF of the background pixels}$$

$$p_2(X) = \text{PDF of the object pixels}$$

'T' is the threshold value which is the default threshold value. If the pixel value specified as less than or equal to T then it belongs to the normal, hence it belongs to the abnormal.

$$f(a,b) > T \rightarrow (a,b) \in \text{object or abnormal cells}$$

$$f(a,b) \leq T \rightarrow (a,b) \in \text{background}$$

Err1-Represents the error if the background pixels are misclassified as abnormal cells.
Err2-Represents the error if the object pixel is misclassified as abnormal cells.

$$\mathrm{Err}_1(\mathrm{T}) = \int_{-\infty}^{\infty} \mathrm{p}_1(\mathrm{X})\mathrm{DZ} \quad (2)$$

$$\mathrm{Err}(\mathrm{T}) = \mathrm{Prob}_2\mathrm{Err}_1(\mathrm{T}) + \mathrm{Prob}_1\mathrm{Err}_2(\mathrm{T}) \quad (3)$$

$$\mathrm{Err}_2(\mathrm{T}) = \int_{\mathrm{T}}^{\infty} \mathrm{p}_2(\mathrm{X})\mathrm{DZ} \quad (4)$$

Err (T): Overall error in the classification of pixels as abnormal cells.

### *3.3 Convolutional Neural Networks (CNN)*

This approach is the combination of CNN and FBDMA to get better output. This is a multi-featured approach that can process complex MRI images to detect tumor cells. After several steps for the processing of MRI brain scan images, the CNN detects the tumors by highlighting the affected regions, and these are classified as cancerous and non-cancerous tumors. These are labeled datasets which are having classes. In this paper, the CNN contains 4 layers such as Conv1, Rectified Linear Unit Layer(ReLu), Pooling Layer(POOL1), and Fully-Connected Layer (FCL).

**Conv1:** It is the initial layer used to extract better features from MRI brain images. Based on the pixel rate of the input images the features used the small square of input data. In this layer, 'N' filters are present which are very small in size such as [3 x 3]. The input image matrix is convoluted by using the sliding window through the height (h) and width (w) of the image. The selected squares of the image are shown by using the feature matrix and this is used to multiply the pixel by pixel. The total number of pixels is shown after the values are added and divided (3x3 filter size). The values that are obtained from this are placed in a new matrix. Without losing any feature this process helps to reduce the size of the image.

$$(\mathrm{a} * \mathrm{b}) = \int_{-\infty}^{\infty} \mathrm{a}(\tau)\mathrm{g}(\mathrm{t} - \tau)\mathrm{d}\tau \quad (5)$$

**Activation function:** These functions measure the weighted sum and add bias to it. This function integrates the non-linearity to the output. The following equation represents this function.

$$f(a) = \frac{e^a}{sum(e^a)} + In\left(\frac{1}{1+e^{-x}}\right) \quad (6)$$

**Pooling Layer:** If the image is large parameters are reduced. There are three types of pooling layers present such as average pooling (AP), L2-norm pooling, and max pooling. The filter size is generally 2 x 2 and also strides of similar length. Then this will apply input volume and a maximum number of outputs of sub-regions that are convolved. In Figure 3, the output steps are explained. Based on the Max-pool values in the image is classified.

**Fully Connected Layers (FCL):** The FCL contains the weights and biases that are integrated with neurons. In FCL all the neurons are interconnected between the layers. All these layers come before the output layer and show the outputs for all the layers.

FC layer takes the input MRI image from previous layer. The flattened vector mainly processes all the FC layers that are taken used in mathematical methods. The classification of images takes place in this stage. All the previous layers connected with the FC achieved better performance compared with a single connected layer. Without any human interference, these layers process the data.

In CNN, the ReLU is integrated and it is represented as:

$$\mathrm{f}(\mathrm{k}) = \max(0, \mathrm{k})$$

Now, the dataset images are classified as tumor and non-tumor as shown in figure 1. The tumor images are given as input to FBDMA Algorithm.

Finally, the cancer cells are identified using FBDMA.

### *3.4 Bilateral Filter*

In a bilateral filter, the Gaussian measures the strong regions among constant color and light color regions. This is also focused on finding the high color deviation. This filter strongly works on the edges of the input image. The Gaussian filter applied at a pixel in image_I can be written in Equation 7

Calculate Bilateral Filter,$\mathrm{G}(\mathrm{p_x})$,

$$\mathrm{G}(\mathrm{p_x}) = \frac{1}{\omega}\sum_{\mathrm{q}\in\mathrm{S}} \mathcal{N}(|\mathrm{a}-\mathrm{b}|)\mathrm{I_b} \quad (7)$$

Initialize the distance between pixel a and b, that is a-b. S represents the nearest neighbor pixels, N- Normal distribution and -normalized factor. Thus the noise filtered image (I) is obtained.

Equation 8 used to measure the pixel intensity in the given input image. This is represented with the square matrix C with size of N x N, where N-No of gray levels. Every {ij} in the matrix is defined as equation 8.

$$C_{ij} = \sum_{a=1}^{W} \sum_{b=1}^{H} 1(I(a,b),i) * 1(I(a + \triangle a, b + \triangle b), j \qquad (8)$$

Where $\triangle a$ and $\triangle b$Defines the relationshipamong the two pixels; W-Width and H-Height of the Image I, 1(I, j) isdefined as

$$I(i,j) = \begin{cases} 1, & \text{if } i = j \\ 0, & \text{otherwise} \end{cases}$$

If I achieved the value 1 then it the pixel intensity is high if it is 0then low pixel intensity.

### *3.5 Identification of Cancer Cells*

A filtered (Noise free) image that contains tumors or classified tumors is taken in each identified region. We calculate the color intensity every pixel in the identified tumor region then this pixel value is compared with the threshold value; if it is less than the threshold value, we color the pixel with dark (black); otherwise, we color the pixel with bright (white) then while the region is identified as probably cancer.
Now, calculate the errors in misclassified pixels.

**Algorithm 1Finding the Intensity of Images to Detect the Cancer Cells**

**Input:** Filtered Image I and Region$R = R_1, R_2, R_3 \ldots \ldots R_n$, Where I=Input Image

**Output:** Classification of Cancer/NoN-Cancer

For each region $R_i$ of Image I do

Calculate high Intensity (W) and Low Intensity (B) using Equation (8) based on threshold

Float threshold = 127; //Global threshold with a value of 127 is applied

For $i = 1$ to $\text{width}(R_i)$ do

For $j = 1$ to $\text{height}(R_i)$do

```
Loc=y+x*columnwidth
If (I[Loc]<threshold)
    Dest[Loc]=0
Else
    Dest[Loc]=255
End for
End for
Return dest
End for
```

## 4. Implementation Results and Discussions

### *4.1 Experimental Setup*

All algorithms were implemented on 11th Gen Intel(R) Core (TM) i5-1135G7 @ 2.40GHz 2.42 GHz, 16.0 GB, 64-bit operating system (OS), x64 based processor with NVIDIA GeForce GTX 1080 GPU on Python Programming Language with the help of powerful library Packages like Pandas, Keras, NumPy, Matplotlib, Seaborn, scikit-learn, etc., The convolutional neural networks were performed and trained using the framework of Pytorch 1.3.0.

The dataset belongs to Br35H and consists of two folders for training and testing. Training consists of 500 non-tumors and 500 tumor images, a total of 1000 training MRI images. The testing folder contains 1000 MRI images and which consist of 600 tumor images, 400 non-tumor images, among tumor images some images are cancerous some are non-cancerous images. By using the following parameters such as sensitivity or recall, accuracy, precision, F1-score, and duration (milliseconds) Apply the confusion matrix to the observed results.

### *4.2 Performance Analysis*

Confusion matrix analysis the performance of FBDMA. It mainly gives the idea about the classification model and whether it shows the right and what type of errors are occurring. This will count all the values that are classified based on the proposed model. The count values are done by using the following variables
TP: The model correctly predicts the positive result (i.e Disease present).

TN: The model correctly predicts the negative result (i.e No disease).
FP: The model incorrectly predicts the positive result.
FN: The model incorrectly predicts the negative result.

**Prediction outcome**

| actual value | p | n | total |
|---|---|---|---|
| p′ | True Positive (TP)[560] | False Negative (FN)[31] | P′ |
| n′ | False Positive (FP)[25] | True Negative (TN)[370] | N′ |
| total | P | N | |

**Accuracy:** It is defined as the sum of all correctly predicted rows divided by the total number of predictions. Here, the errors are also important to get the accurate results about the model.

$$\text{Accuracy} = \frac{\text{TP} + \text{TN}}{\text{TP} + \text{TN} + \text{FP} + \text{FN}}$$

**Precision:** This measures overall predictions obtained from model are originally positive from all positive predictions.

$$\text{Precision} = \frac{\text{TP}}{\text{TP} + \text{FP}}$$

**Recall:** This shows huge impact on output. This will correctly predict the positives from actual positives.

$$\text{Recall} = \frac{\text{TP}}{\text{TP} + \text{FP}}$$

**F1-Score:** It is the symphonious mean of precision and recall. The best value of F1 score is 1 and worst value is 0.

$$\text{F1} = \frac{2 * \text{Precision} * \text{Recall}}{\text{Precision} + \text{Recall}} = \frac{2 * \text{TP}}{2 * \text{TP} + \text{FP} + \text{FN}}$$

Error Rate: This shows overall errors occurred at the time of classification.

$$\textbf{Error Rate} = \frac{\textbf{FP+FN}}{\textbf{TP+TN+FP+FN}}$$

Table 2: The performance of Algorithms for Training of Br35H Dataset for the Brain Tumor MRI Images

| Algorithms | Recall | Accuracy | Precision | F1-Score |
|---|---|---|---|---|
| ConvML | 56.23 | 61.34 | 65.12 | 53.43 |
| Hybrid Model | 71.23 | 74.78 | 71.89 | 71.98 |
| FBDMA | 94.34 | 96.78 | 97.32 | 98.12 |

In table 2 the performance of algorithms based on training is given with the following parameters. These algorithms are applied to the Br35H dataset collected from Kaggle. The performance of FBDMA shows an accuracy of 96.78, recall is 94.34, precision is 97.32 and F1-score is 98.12. It is better than existing system.

Table 3 shows the overall computation time of the existing and proposed algorithms. The computation time is called as duration (sec). The FBDMA shows less duration compared with existing approaches.

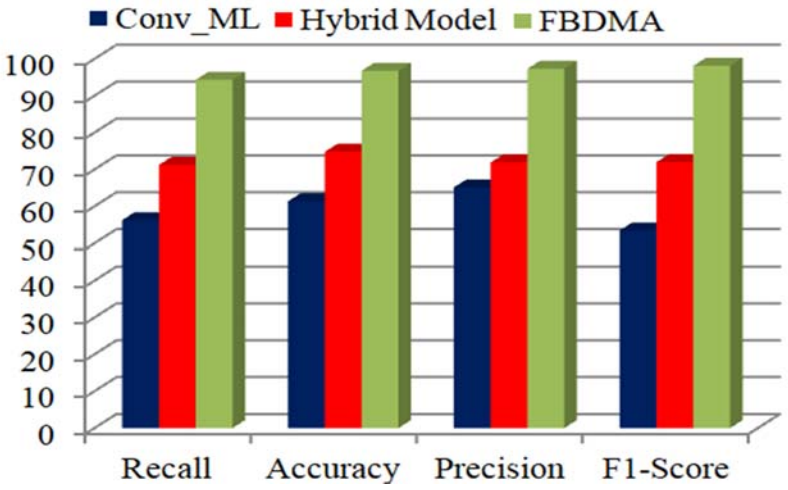


Fig. 4. Performance on training of Br35H Dataset for the Brain Tumor MRI Images

Table 3: Performance based on Computation and Error rate for Brain Tumor Detection

| Algorithm | Duration (Sec) | Error Rate (%) |
|---|---|---|
| Conv_ML | 17.89 | 12.45 |
| Hybrid Model | 13.23 | 9.45 |
| FBDMA | 9.23 | 5.65 |

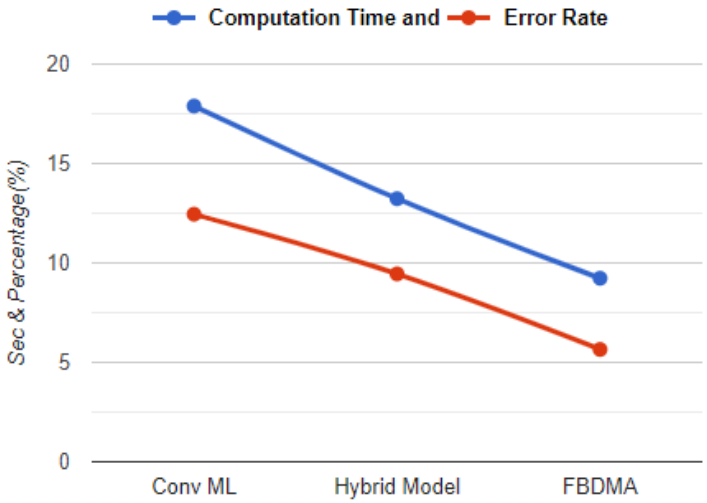


Fig. 5. Graph representation for measuring computation time(Sec) for Training of Brain Tumor MRI Images

In table 4 the performance of algorithms based on testing is given with the following parameters. These algorithms are applied to the Br35H dataset collected from Kaggle. The performance of FBDMA shows an accuracy of 97.98, recall is 96.78, precision is 98.34 and F1-score is 98.76. It is better than existing system.

Table 5 shows the overall computation time of the existing and proposed algorithms. The computation time is called as duration (sec). The FBDMA shows less duration compared with existing approaches.

Table 4: The performance of Algorithms for Testing of Br35H Dataset for the Brain Tumor MRI Images

| Algorithms | Recall | Accuracy | Precision | F1-Score |
|---|---|---|---|---|
| ConvML | 58.98 | 59.67 | 61.23 | 61.98 |
| Hybrid Model | 82.45 | 80.45 | 81.23 | 82.56 |
| FBDMA | 96.78 | 97.98 | 98.34 | 98.76 |

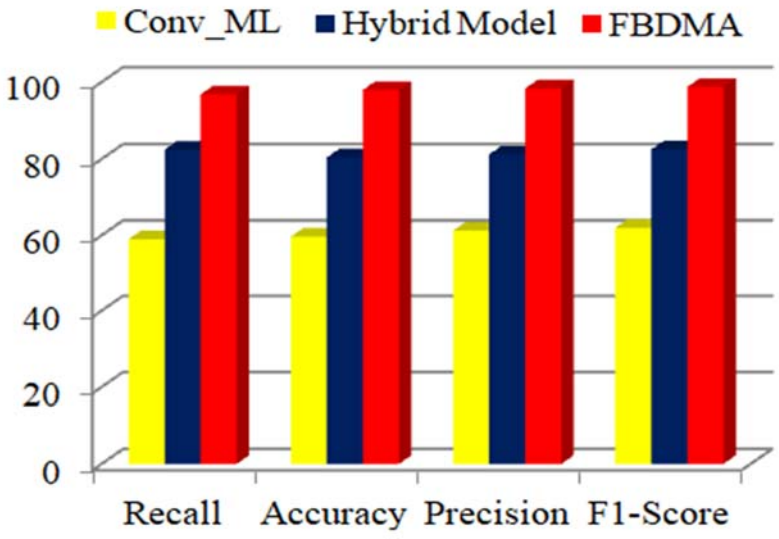


Fig. 6. Performance of Testing of Br35H Dataset for the Brain Tumor MRI Images

Table 5: Performance based on Duration and Error Rate for Tumor Detection

| Algorithm | Duration (Sec) | Error Rate (%) |
|---|---|---|
| Conv_ML | 19.34 | 14.23 |
| Hybrid Model | 15.76 | 11.34 |
| FBDMA | 10.56 | 8.56 |

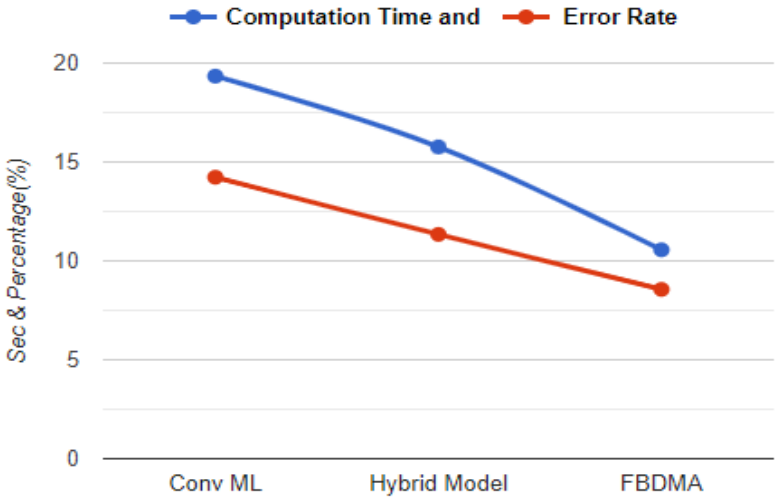


Fig. 7. Graph representation for measuring computation time(Sec) for Testing of Brain Tumor MRI Images

In table 6 the performance of algorithms based on training is given with the following parameters. These algorithms are applied to the Br35H dataset for cancer tumor MRI images collected from Kaggle. The performance of these algorithms shows an accuracy of 98.34, recall is 96.12, precision is 98.67 and F1-score is 98.56.

Table 7 shows the overall computation time of the existing and proposed algorithms. The computation time is called as duration (sec). The FBDMA shows less duration compared with existing approaches.

Table 6: The performance of Algorithms for Training of Br35H Dataset for the Cancer Tumor MRI Images

| Algorithms | Recall | Accuracy | Precision | F1-Score |
|---|---|---|---|---|
| ConvML | 62.67 | 64.12 | 65.12 | 65.41 |
| Hybrid Model | 83.56 | 82.45 | 82.56 | 83.56 |
| FBDMA | 96.12 | 98.34 | 98.67 | 98.56 |

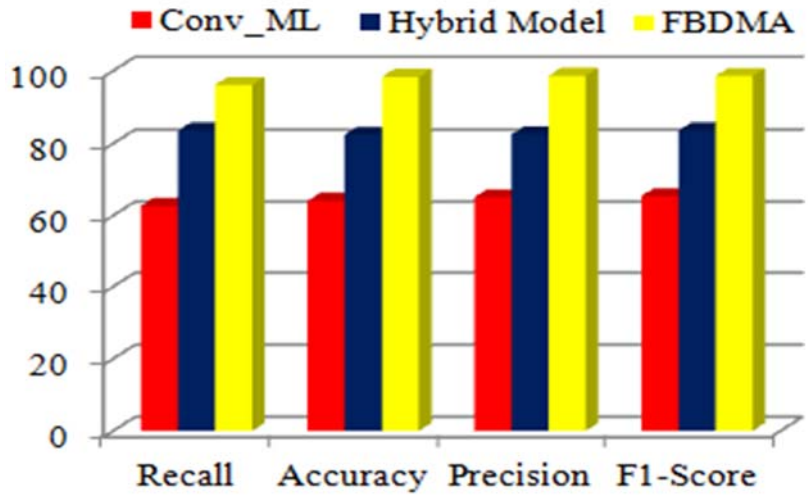


Fig. 8. Performance of Algorithms for Training of Br35H Dataset for the Cancer Tumor MRI Images

Table 7: Performance based on Duration and Error Rate for the Cancer Tumor MRI Images

| Algorithm | Duration (Sec) | Error Rate (%) |
|---|---|---|
| Conv_ML | 23.56 | 13.56 |
| Hybrid Model | 14.97 | 9.56 |
| FBDMA | 8.78 | 5.23 |

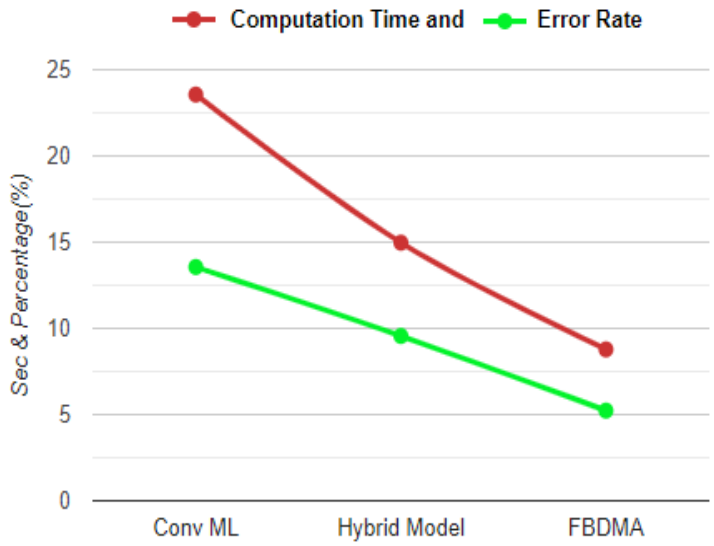


Fig. 9. Graph representation for measuring computation time(Sec) for Training on Cancer and Tumor MRI Images

In table 8 the performance of algorithms based on testing is given with the following parameters. These algorithms are applied to the Br35H dataset for cancer tumor MRI images collected from Kaggle. The performance of these algorithms shows an accuracy of 98.56, recall is 97.89, precision is 98.78 and F1-score is 98.12.

Table 9 shows the overall computation time of the existing and proposed algorithms. The computation time is called as duration (sec). The FBDMA shows less computation compared with existing approaches.

Table 8: The performance of Algorithms for Testing of Br35H Dataset for the Cancer Tumor MRI Images

| Algorithms | Recall | Accuracy | Precision | F1-Score |
|---|---|---|---|---|
| ConvML | 63.45 | 65.78 | 67.56 | 65.78 |
| Hybrid Model | 85.12 | 84.67 | 86.23 | 87.12 |
| FBDMA | 97.89 | 98.56 | 98.78 | 98.12 |

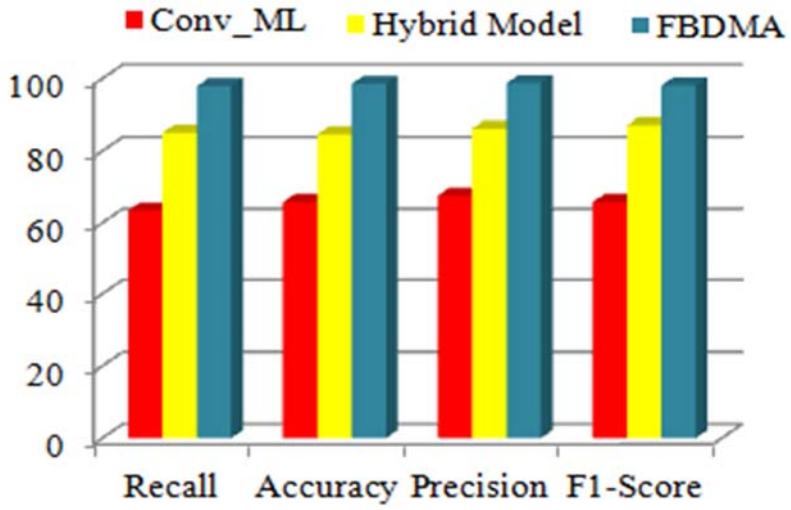


Fig. 10. Performance of Algorithms for testing of Br35H Dataset for the Cancer Tumor MRI Images

Table 9: Performance based on Duration and Error Rate for the Cancer Tumor MRI Images

| Algorithm | Duration (Sec) | Error Rate (%) |
|---|---|---|
| Conv_ML | 24.34 | 12.89 |
| Hybrid Model | 15.87 | 9.89 |
| FBDMA | 7.56 | 5.21 |

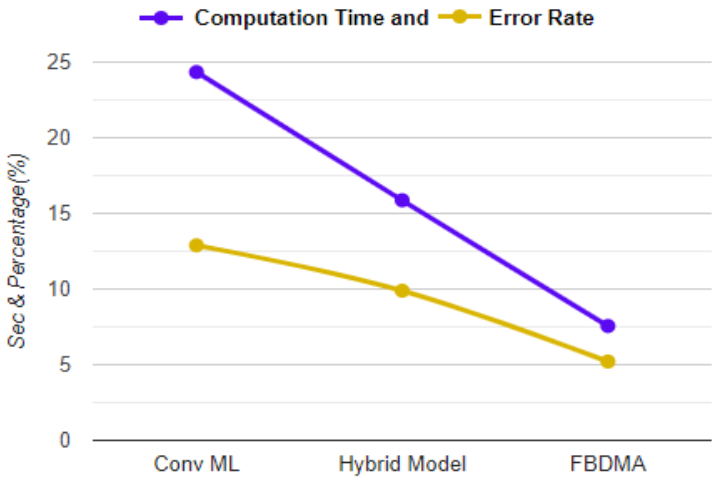


Fig. 11. Graph representation for measuring computation time(Sec) and Error rate for Testing on Cancer and Tumor Images

Figure 12, 13, and 14 describes the process of detecting and diagnosing the MRI brain tumor image. An Optimal thresholding is used to remove the noise from input image. Noise removal shows a significant impact on output. After this step, the segmented image is partitioned. The noise removal image is considered the input, and edge detection is applied to find the MRI images' accurate edges. Figure (d) shows the highlighted part with red color, which affected the tumor region.

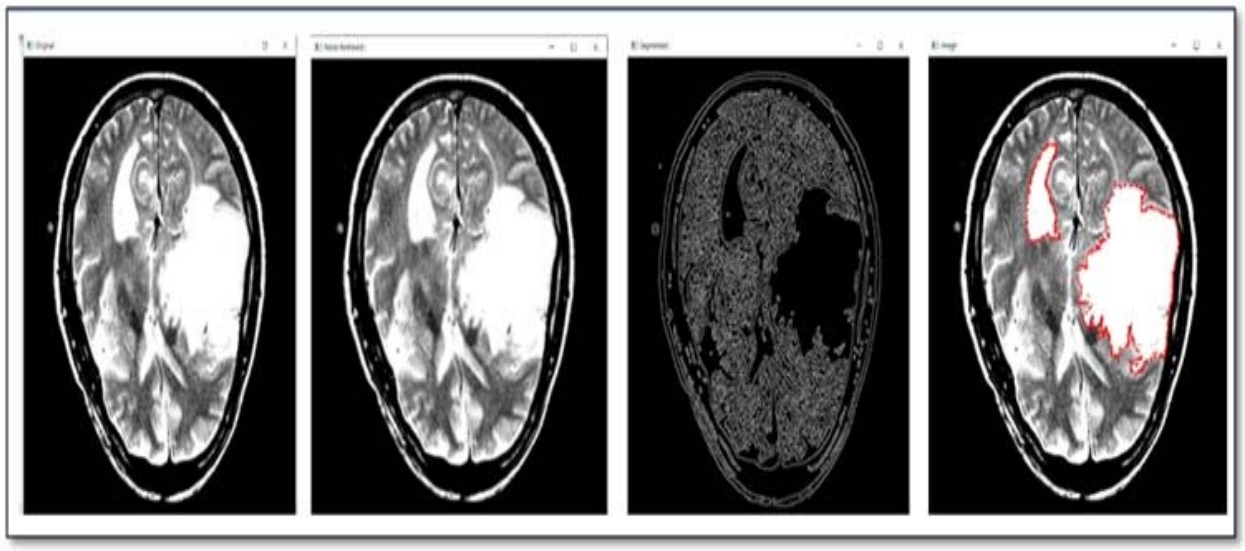

Fig. 12. (A)Normal Image (B)Noise Filter Image (C)Edge Detection and Segmented Image (D)Tumor Region Detection

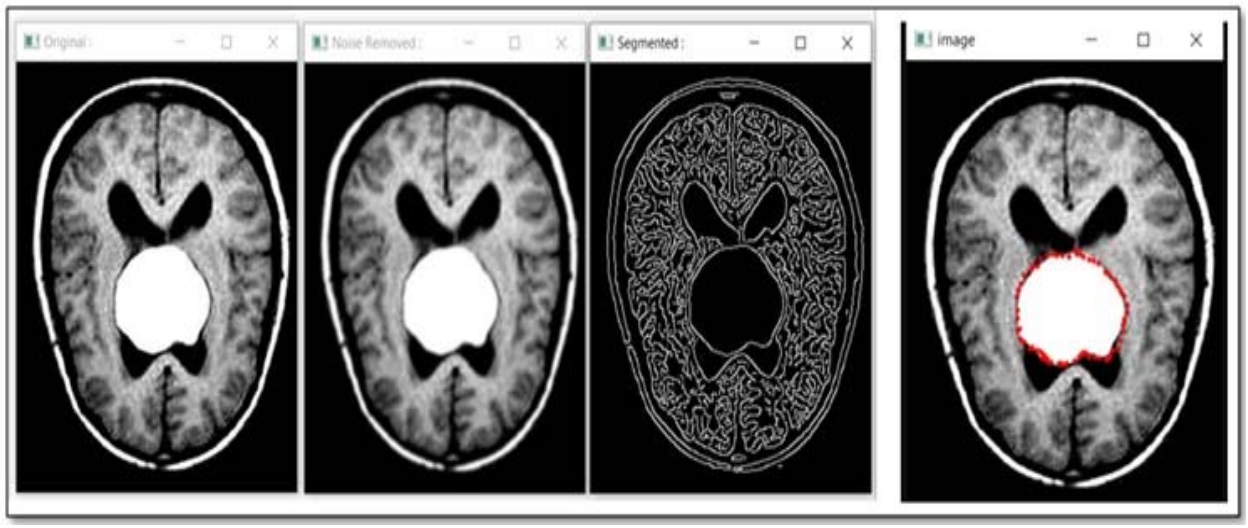


Fig. 13. (A) Normal Image (B) Noise Filter Image (C) Edge Detection and Segmented Image (D) Tumor (Red Color)

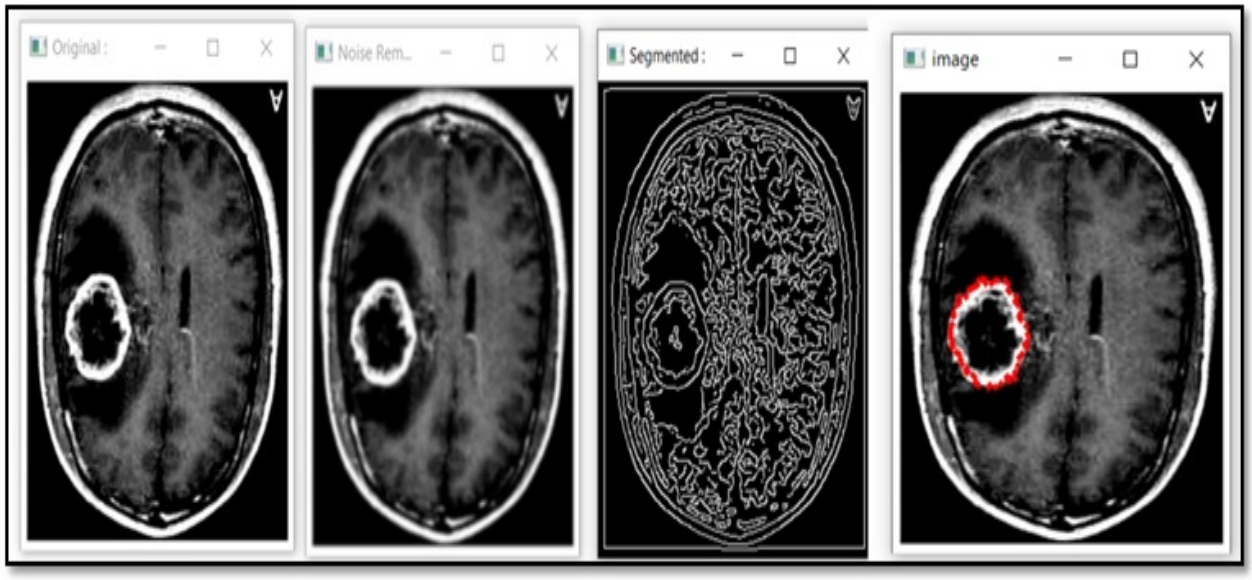


Fig. 14. (A) Normal Image (B) Noise Filter Image (C) Edge Detection and Segmented Image (D) Tumor (Red Color)

Figure 15,16, and 17 describes the process of identifying the cancer cells in MRI brain tumor regions. The cancer cells considered as high intensity regions. Figure (d) shows the highlighted part with red color which is the affected tumor region and blue color represented the cancerous region. The FBDMA is applied in the last step to find whether the tumor is cancerous or not.

The tables and figures were obtained using Python code with the proposed MRI brain images. The performance is analyzed based on training and testing.

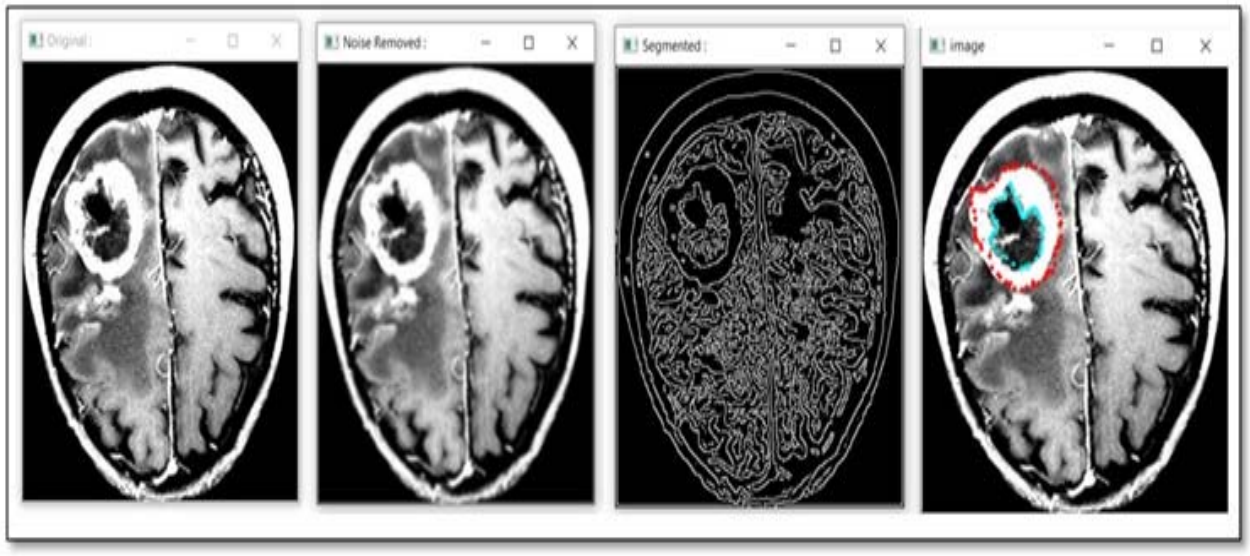


Fig. 15. (A) Normal Image (B) Noise Filter Image (C) Edge Detection and Segmented Image (D) Tumor (Red Color) and Blue color represent the Cancerous Cells

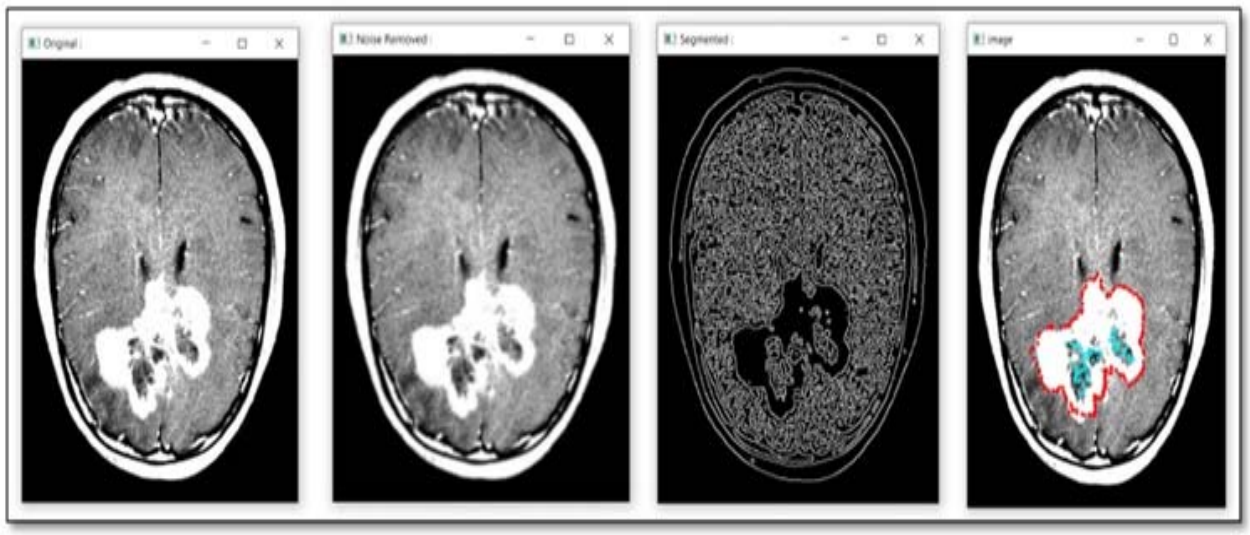


Fig. 16. (A) Normal Image (B) Noise Filter Image (C) Edge Detection and Segmented Image (D) Tumor (Red Color) and Blue color represent the Cancerous Cells

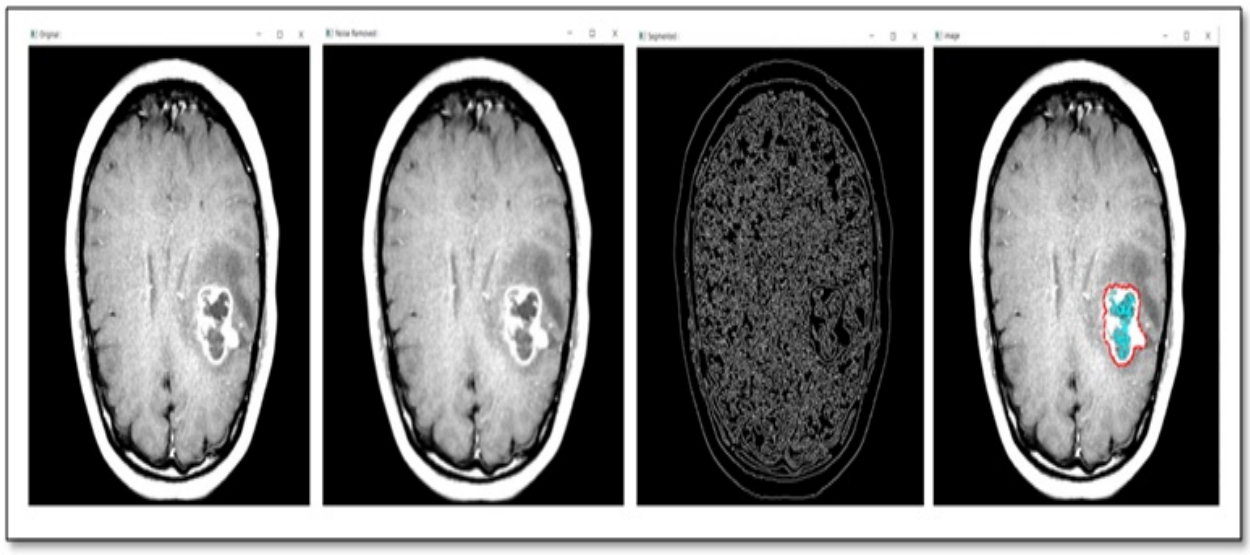

Fig. 17. (A) Normal Image (B) Noise Filter Image (C) Edge Detection and Segmented Image (D) Tumor (Red Color) and Blue color represent the Cancerous Cells

## 5. Conclusion

The proposed system in this paper focused on detecting and diagnosing tumor cells and cancer cells present in the human brain by using MRI scan images. FBDMA is the integrated approach that is combined with the VGG19 as a pre-trained model for effective training and also for feature extraction. The photon noise is identified and it is removed with the Bilateral Filters from the MRI brain images. Optimal threshold Segmentation is utilized to find normal and abnormal regions from the given input images. Based on the threshold values the regions are classified as tumors and cancerous tumors. CNN is also used for the extraction of features by testing MRI brain images and shows the tumors and cancerous tumors. The performance of the tumor and cancerous detection is approximately 98.67 accuracy compared with Conv-ML and hybrid approach. The FBDMA is used to classify tumors and cancerous. Tumors regions are represented in red color and cancerous regions are represented in blue color. The average processing time for every image for detecting the tumor region and cancerous region is about 9.78 Sec.

## Funding

No funding is provided for the preparation of manuscript.

## Conflicts of interest

The authors have no conflicts of interest to declare.

## References

[1] A. Sekhar, S. Biswas, R. Hazra, A. K. Sunaniya, A. Mukherjee and L. Yang, "Brain Tumor Classification Using Fine-Tuned GoogLeNet Features and Machine Learning Algorithms: IoMT Enabled CAD System," in IEEE Journal of Biomedical and Health Informatics, vol. 26, no. 3, pp. 983-991, March 2022, doi: 10.1109/JBHI.2021.3100758.

[2] K. Muhammad, S. Khan, J. D. Ser and V. H. C. d. Albuquerque, "Deep Learning for Multigrade Brain Tumor Classification in Smart Healthcare Systems: A Prospective Survey," in IEEE Transactions on Neural Networks and Learning Systems, vol. 32, no. 2, pp. 507-522, Feb. 2021, doi: 10.1109/TNNLS.2020.2995800.

[3] K. Davagdorj, J. -W. Bae, V. -H. Pham, N. Theera-Umpon and K. H. Ryu, "Explainable Artificial Intelligence Based Framework for Non-Communicable Diseases Prediction," in IEEE Access, vol. 9, pp. 123672-123688, 2021, doi: 10.1109/ACCESS.2021.3110336.

[4] H. Yin and N. K. Jha, "A Health Decision Support System for Disease Diagnosis Based on Wearable Medical Sensors and Machine Learning Ensembles," in IEEE Transactions on Multi-Scale Computing Systems, vol. 3, no. 4, pp. 228-241, 1 Oct.-Dec. 2017, doi: 10.1109/TMSCS.2017.2710194.

[5] Z. N. K. Swati et al., "Content-based brain tumor retrieval for MR images using transfer learning", IEEE Access, vol. 7, pp. 17809-17822, 2019.

[6] P. Pace, G. Aloi, R. Gravina, G. Caliciuri, G. Fortino and A. Liotta, "An edge-based architecture to support efficient applications for healthcare industry 4.0", IEEE Trans. Ind. Informat., vol. 15, no. 1, pp. 481-489, Jan. 2019.

[7] M. Mardani et al., "Deep generative adversarial neural networks for compressive sensing MRI", IEEE Trans. Med. Imag., vol. 38, no. 1, pp. 167-179, Jan. 2019.

[8] Z. Jia and D. Chen, "Brain Tumor Identification and Classification of MRI images using deep learning techniques," in IEEE Access, doi: 10.1109/ACCESS.2020.3016319.

[9] M. Ali, S. O. Gilani, A. Waris, K. Zafar and M. Jamil, "Brain Tumour Image Segmentation Using Deep Networks," in IEEE Access, vol. 8, pp. 153589-153598, 2020, doi: 10.1109/ACCESS.2020.3018160.

[10] M. S. Majib, M. M. Rahman, T. M. S. Sazzad, N. I. Khan and S. K. Dey, "VGG-SCNet: A VGG Net-Based Deep Learning Framework for Brain Tumor Detection on MRI Images," in IEEE Access, vol. 9, pp. 116942-116952, 2021, doi: 10.1109/ACCESS.2021.3105874.
[11] Y. Zhang, M. Qiu, C.-W. Tsai, M. M. Hassan, and A. Alamri, "HealthCPS: Healthcare cyberphysical system assisted by cloud and big data," IEEE Syst. J., vol. 11, no. 1, pp. 88–95, Mar. 2017.
[12] S. Trajanovski, C. Shan, P. J. C. Weijtmans, S. G. B. de Koning and T. J. M. Ruers, "Tongue Tumor Detection in Hyperspectral Images Using Deep Learning Semantic Segmentation," in IEEE Transactions on Biomedical Engineering, vol. 68, no. 4, pp. 1330-1340, April 2021, doi: 10.1109/TBME.2020.3026683.
[13] D. Hyun, L. Abou-Elkacem, R. Bam, L. L. Brickson, C. D. Herickhoff and J. J. Dahl, "Nondestructive Detection of Targeted Microbubbles Using Dual-Mode Data and Deep Learning for Real-Time Ultrasound Molecular Imaging," in IEEE Transactions on Medical Imaging, vol. 39, no. 10, pp. 3079-3088, Oct. 2020, doi: 10.1109/TMI.2020.2986762.
[14] D. Krijgsman et al., "Quantitative Whole Slide Assessment of Tumor-Infiltrating CD8-Positive Lymphocytes in ER-Positive Breast Cancer in Relation to Clinical Outcome," in IEEE Journal of Biomedical and Health Informatics, vol. 25, no. 2, pp. 381-392, Feb. 2021, doi: 10.1109/JBHI.2020.3003475.
[15] Y. Xie et al., "Knowledge-based Collaborative Deep Learning for Benign-Malignant Lung Nodule Classification on Chest CT," in IEEE Transactions on Medical Imaging, vol. 38, no. 4, pp. 991-1004, April 2019, doi: 10.1109/TMI.2018.2876510.
[16] A. S. Musallam, A. S. Sherif and M. K. Hussein, "A New Convolutional Neural Network Architecture for Automatic Detection of Brain Tumors in Magnetic Resonance Imaging Images," in IEEE Access, vol. 10, pp. 2775-2782, 2022, doi: 10.1109/ACCESS.2022.3140289.
[17] S. E. Divel and N. J. Pelc, "Accurate Image Domain Noise Insertion in CT Images," in IEEE Transactions on Medical Imaging, vol. 39, no. 6, pp. 1906-1916, June 2020, doi: 10.1109/TMI.2019.2961837.
[18] P. Kumar Mallick, S. H. Ryu, S. K. Satapathy, S. Mishra, G. N. Nguyen and P. Tiwari, "Brain MRI Image Classification for Cancer Detection Using Deep Wavelet Autoencoder-Based Deep Neural Network," in IEEE Access, vol. 7, pp. 46278-46287, 2019, doi: 10.1109/ACCESS.2019.2902252.
[19] N. Noreen, S. Palaniappan, A. Qayyum, I. Ahmad, M. Imran and M. Shoaib, "A Deep Learning Model Based on Concatenation Approach for the Diagnosis of Brain Tumor," in IEEE Access, vol. 8, pp. 55135-55144, 2020, doi: 10.1109/ACCESS.2020.2978629.
[20] A. Gumaei, M. M. Hassan, M. R. Hassan, A. Alelaiwi and G. Fortino, "A Hybrid Feature Extraction Method With Regularized Extreme Learning Machine for Brain Tumor Classification," in IEEE Access, vol. 7, pp. 36266-36273, 2019, doi: 10.1109/ACCESS.2019.2904145.
[21] M. Li, L. Kuang, S. Xu and Z. Sha, "Brain Tumor Detection Based on Multimodal Information Fusion and Convolutional Neural Network," in IEEE Access, vol. 7, pp. 180134-180146, 2019, doi: 10.1109/ACCESS.2019.2958370.
[22] X. Dong, Y. Zhou, L. Wang, J. Peng, Y. Lou and Y. Fan, "Liver Cancer Detection Using Hybridized Fully Convolutional Neural Network Based on Deep Learning Framework," in IEEE Access, vol. 8, pp. 129889-129898, 2020, doi: 10.1109/ACCESS.2020.3006362.
[23] M. S. Majib, M. M. Rahman, T. M. S. Sazzad, N. I. Khan and S. K. Dey, "VGG-SCNet: A VGG Net-Based Deep Learning Framework for Brain Tumor Detection on MRI Images," in IEEE Access, vol. 9, pp. 116942-116952, 2021, doi: 10.1109/ACCESS.2021.3105874.
[24] P. Khan et al., "Machine Learning and Deep Learning Approaches for Brain Disease Diagnosis: Principles and Recent Advances," in IEEE Access, vol. 9, pp. 37622-37655, 2021, doi: 10.1109/ACCESS.2021.3062484.
[25] A. Anaya-Isaza and L. Mera-Jiménez, "Data Augmentation and Transfer Learning for Brain Tumor Detection in Magnetic Resonance Imaging," in IEEE Access, vol. 10, pp. 23217-23233, 2022, doi: 10.1109/ACCESS.2022.3154061.
[26] Y. Zhang et al., "Deep Learning Initialized and Gradient Enhanced Level-Set Based Segmentation for Liver Tumor From CT Images," in IEEE Access, vol. 8, pp. 76056-76068, 2020, doi: 10.1109/ACCESS.2020.2988647.
[27] Z. Zhang and Y. Han, "Detection of Ovarian Tumors in Obstetric Ultrasound Imaging Using Logistic Regression Classifier With an Advanced Machine Learning Approach," in IEEE Access, vol. 8, pp. 44999-45008, 2020, doi: 10.1109/ACCESS.2020.2977962.
[28] M. Valkonen et al., "Cytokeratin-Supervised Deep Learning for Automatic Recognition of Epithelial Cells in Breast Cancers Stained for ER, PR, and Ki-67," in IEEE Transactions on Medical Imaging, vol. 39, no. 2, pp. 534-542, Feb. 2020, doi: 10.1109/TMI.2019.2933656.
[29] C.-M. Feng, Y. Xu, J.-X. Liu, Y.-L. Gao and C.-H. Zheng, "Supervised discriminative sparse PCA for com-characteristic gene selection and tumor classification on multiview biological data", IEEE Trans. Neural Netw. Learn. Syst., vol. 30, no. 10, pp. 2926-2937, Oct. 2019.
[30] J. Sun, C. Li, X.-J. Wu, V. Palade and W. Fang, "An effective method of weld defect detection and classification based on machine vision", IEEE Trans. Ind. Informat., vol. 15, no. 12, pp. 6322-6333, Dec. 2019.
[31] Y. Shi, H.-I. Suk, Y. Gao, S.-W. Lee and D. Shen, "Leveraging coupled interaction for multimodal Alzheimer's disease diagnosis", IEEE Trans. Neural Netw. Learn. Syst., vol. 31, no. 1, pp. 186-200, Jan. 2020.
[32] X. Bai, Y. Zhang, H. Liu and Z. Chen, "Similarity measure-based possibilistic FCM with label information for brain MRI segmentation", IEEE Trans. Cybern., vol. 49, no. 1, pp. 2618-2630, Jul. 2019.
[33] M. A. Ottom, H. A. Rahman and I. D. Dinov, "Znet: Deep Learning Approach for 2D MRI Brain Tumor Segmentation," in IEEE Journal of Translational Engineering in Health and Medicine, vol. 10, pp. 1-8, 2022, Art no. 1800508, doi: 10.1109/JTEHM.2022.3176737.
[34] S. Asif, W. Yi, Q. U. Ain, J. Hou, T. Yi and J. Si, "Improving Effectiveness of Different Deep Transfer Learning-Based Models for Detecting Brain Tumors From MR Images," in IEEE Access, vol. 10, pp. 34716-34730, 2022, doi: 10.1109/ACCESS.2022.3153306.
[35] N. Noreen, S. Palaniappan, A. Qayyum, I. Ahmad, M. Imran and M. Shoaib, "A deep learning model based on concatenation approach for the diagnosis of brain tumor", IEEE Access, vol. 8, pp. 55135-55144, 2020.
[36] S. Ahmad and P. K. Choudhury, "On the Performance of Deep Transfer Learning Networks for Brain Tumor Detection Using MR Images," in IEEE Access, vol. 10, pp. 59099-59114, 2022, doi: 10.1109/ACCESS.2022.3179376.
[37] Q. Hao et al., "Fusing Multiple Deep Models for In Vivo Human Brain Hyperspectral Image Classification to Identify Glioblastoma Tumor," in IEEE Transactions on Instrumentation and Measurement, vol. 70, pp. 1-14, 2021, Art no. 4007314, doi: 10.1109/TIM.2021.3117634.
[38] H. A. Shah, F. Saeed, S. Yun, J. -H. Park, A. Paul and J. -M. Kang, "A Robust Approach for Brain Tumor Detection in Magnetic Resonance Images Using Finetuned EfficientNet," in IEEE Access, vol. 10, pp. 65426-65438, 2022, doi: 10.1109/ACCESS.2022.3184113.\
[39] A. H. Abdel-Gawad, L. A. Said and A. G. Radwan, "Optimized Edge Detection Technique for Brain Tumor Detection in MR Images," in IEEE Access, vol. 8, pp. 136243-136259, 2020, doi: 10.1109/ACCESS.2020.3009898.
[40] Z. A. Al-Saffar and T. Yildirim, "A Novel Approach to Improving Brain Image Classification Using Mutual Information-Accelerated Singular Value Decomposition," in IEEE Access, vol. 8, pp. 52575-52587, 2020, doi: 10.1109/ACCESS.2020.2980728.

**Authors Profile**

P. Durga (Putta Durga) earned her undergraduate degree from Chadalawada Ramanamma Engineering College, Tirupati, JNTUA, and her Master's degree in Computer Science and Engineering from SRK Institute of Technology, Vijayawada, JNTUK, Andhra Pradesh, India. She is having four years of experience in teaching and presently she is pursuing a Ph.D. degree in the School of Computer Science & Engineering (SCOPE), Vellore Institute of Technology (VIT–AP), Amaravati, Andhra Pradesh, India. Her current research interests are in the area of Decision Making, Deep Learning, Digital Image Processing, and Machine Learning.

Dr. T. Sudhakar, Received his B.E and M.E. degrees in Computer Science and Engineering discipline in the years 2002 and 2005 respectively. He received his Ph.D. degree from the Faculty of Information and Communication Engineering, Anna University, Chennai in 2020. He is currently working as an Associate Professor at the School of Computer Science and Engineering, VIT-AP University, Amaravati, Andhra Pradesh, India. He has 17 years of teaching experience and 8 years of research experience. He has published a number of quality research articles in various reputed international journals and conferences. His research interests include Cryptography and Network security, Design of security protocols, Cyber Security, Digital Image Processing and Deep Learning.